NONLINEAR SOIL-PILE INTERACTION ANALYSIS USING A RATIONAL WINKLER SPRING METHOD

Hossein Tahghighi[1] and Kazuo Konagai[2]

Abstract: A simplified computational analogy is being presented in this paper. The model is capable of handling not only the linear but also nonlinear behavior of soil-pile interaction analysis. Despite simplification involved in modeling such complex phenomena, yet the proposed nonlinear soil model can reproduce the system behavior computed by more rigorous three dimensional finite element methods. Therefore the model may be conveniently incorporated as a tool in the practical design of pile foundations.

Key Words: Soil-Pile group interaction, Elastoplastic Winkler hypothesis, three dimensional FEM

Introduction

Evaluation of soil-pile-structure interaction is necessary for a rational seismic design of civil-infrastructures. Such studies can be done experimentally, theoretically or numerically. Various tools have been developed for the analysis of soil-foundation-structure interaction.

As for piles, the static group effect was put on a rational basis, relying on continuum mechanics, by Poulos et al. (1971). For describing dynamic pile group effect, the thin layer element method, TLEM, was first developed by Tajimi and Shimomura (1976) etc. Boundary element solutions for soil-pile systems were formulated by Kaynia et al. (1982) and Banerjee et al. (1987). Though rigorous, these methods are only for analyzing elastic behaviors of soils and structures. With the rapid development of computer technology, a variety of straightforward methods are available for solving problems of increasing complexity. They include Finite Element Methods (FEM) developed by Kimura et al. (2000), Wakai et al. (1999) and Yang et al. (2003). Direct methods, however, require both soils and structures to be treated with equal rigor, and complex variations of soil profile in a 3D expanse should be provided for the analysis. Hence, there yet remains an important place for simple approaches even in these days of highly manipulative numerical solutions to difficult problems. A simple model developed by Nogami and Konagai (1992) hypothesizes that a plane strain slice of side soil determines the side soil stiffness. With this approach, one can cut a distinct side soil spring in half, one for the near field, and the other for the far field that is not strongly affected by the presence of the pile (See Fig. 1). However, a problem for this model is that the impedance function for the elastic side soil converges on zero for static loading. Moreover, its dynamic stiffness near the ground surface is overestimated because the effect of stress free surface is completely ignored assuming a plane strain condition. However, by virtue of its simplicity, there remains a strong need for a Winkler model.

In the present method, the diagonal terms of the exact soil impedance matrix define the elastic side-soil springs of Winkler type. The effect of the off-diagonal terms of the matrix is represented by an additional displacement vector, which is applied to the other ends of the Winkler side-soil springs. The displacement vector is introduced herein as a function of the pile's active length, which was found to be less dependent on the other secondary factors.

Modified Winkler Model

Recently, the second author developed a simplified approach, in which a group of piles is viewed as an equivalent single upright beam [Konagai et. al. 2000], the idea based on the fact that a group of piles often trap soil among them as observed when pulled out [Railway Technology Research Institute 1995]. The upright single beam is a composite of n_p piles and the soil caught among them (Figure 2). The broken line in Figure 2a circumscribing the outermost piles in the group determines its cross section A_G. The soil-pile composite together with its exterior soil is divided into n_L horizontal slices as shown in Figure 2b. The idea has been verified in both linear and nonlinear soil-pile interaction analyses [Konagai et. al. 2002, Konagai et. al. 2003].

[1] PhD. candidate, Institute of Industrial Science, University of Tokyo
[2] Professor, Institute of Industrial Science, University of Tokyo

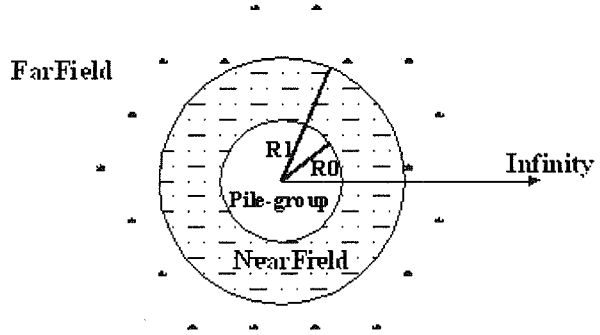

Fig. 1. Schematic view of the Winkler side soil spring

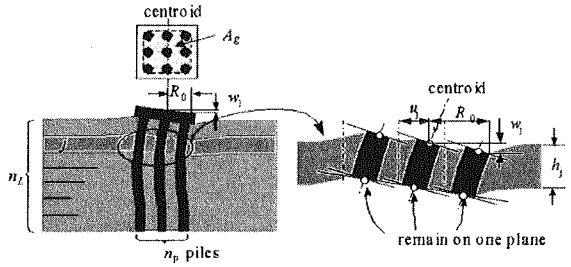

Fig. 2. Assumption for single beam analogy

When the pile group in Fig. 2 is subjected to lateral displacements along its depth, the equation of equilibrium for soil-pile system is written as:

$$\{F_{ext}\} + [\mathbf{K}_{pile}]\{\mathbf{u}_{pile}\} + [\mathbf{K}_{soil}]\{\{\mathbf{u}_{pile}\} - \{\mathbf{u}_{free}\}\} = 0 \tag{1}$$

where, vector $\{F_{ext}\}$ denotes the external load on the pile cap from the superstructure and $\{u_{free}\}$ is the free field ground motions. From the Eq. (1), lateral soil reaction forces on the pile group is written in the following form as:

$$\{\mathbf{p}_{pile}\} = \left|[\mathbf{K}_{soil}]\{\{\mathbf{u}_{pile}\} - \{\mathbf{u}_{free}\}\}\right| \tag{2}$$

Extracting diagonal terms $k_j \ (j = 1,2,\cdots n)$ of the side soil stiffness matrix $[\mathbf{K}_{soil}]$, Equation (2) is rewritten as:

$$\{\mathbf{p}_{pile}\} = \{k_1 u_{pile,1} \quad k_2 u_{pile,2} \quad \cdots \quad k_n u_{pile,n}\}^T - \{\mathbf{p}_{off-diag}\} \tag{3}$$

with

$$\{\mathbf{p}_{off-diag}\} = \text{Off diagonal terms of } [\mathbf{K}_{soil}]\{\mathbf{u}_{pile}\} - [\mathbf{K}_{soil}]\{\mathbf{u}_{free}\} \tag{4}$$

Equation (3) yields the following expression as:

$$\{\mathbf{p}_{pile}\} = \begin{bmatrix} k_1 & 0 & \cdots & 0 \\ 0 & k_2 & & 0 \\ \vdots & & \ddots & \vdots \\ 0 & 0 & \cdots & k_{n_1} \end{bmatrix} \{\{\mathbf{u}_{pile}\} - \{\mathbf{u}_{far}\}\} \tag{5}$$

With $\{\mathbf{u}_{far}\} = \left\{\frac{\{\mathbf{p}_{off-diag}\}}{k_i}\right\}$ (6)

Equation (5) indicates that a Winkler model can describe the soil-pile interaction. Differing from the conventional Winkler model, Eq. (5) shows the necessity of subtracting a displacement vector $\{\mathbf{u}_{far}\}$ from $\{\mathbf{u}_{pile}\}$. The displacement vector $\{\mathbf{u}_{far}\}$ is interpreted as the displacements given on the other ends of the Winkler side-soil springs, and therefore, will be referred to as the "far-end displacements". The side soil stiffness matrix in equation (4) together with $\{\mathbf{u}_{pile}\}$ determines the far-end displacements $\{\mathbf{u}_{far}\}$. The pile-group stiffness matrix includes two stiffness parameters, EI_{sway} and EI_{rock} for the grouped piles, and shear modulus of soil μ [Konagai et. al. 2000]. The first parameter EI_{sway} governs the sway motion of the beam is the product of the bending stiffness of an individual pile EI_{single} and the number of piles n_p, and therefore EI_{sway} and μ are crucial parameters for determining the far-end displacement vector $\{\mathbf{u}_{far}\}$. When a pile group is laterally displaced, the horizontal deflection of the pile group decreases with increasing depth. In practice, most laterally loaded piles are indeed 'flexible' in the sense that they are not deformed over their entire length L. Instead, pile deflections become negligible below an ac tive length (or effective length) L_a. The active length L_a depends largely on these parameters EI_{sway} z z and μ. The above consideration leads to an idea that the far-field displacement vector $\{\mathbf{u}_{far}\}$ will be expressed uniquely in terms of the active pile length L_a.

Far-end soil displacement $\{\mathbf{u}_{far}\}$

To verify the present idea for the far-end soil displacements, $\{\mathbf{u}_{far}\}$, some representative cases were examined. The soil medium was assumed to be a horizontally stratified infinite deposit with material damping of the frequency-independent hysteretic type. Necessary parameters for the examined cases are listed in Table 1. The pile groups examined included 2 × 2, 3 × 3 and 4 × 4 piles (N4, N9 and N16) with the space–diameter ratio s/d set at 2, 3 and 5.

	Young Modulus E(GPa)	Poisson ratio ν	Unit weight γ (KN/m^3)	Friction angle ϕ (deg)	Cohesion C(GPa)	Length L(m)	Diameter d(m)
Pile	50	---------	24.5	--------	-------	15	1.0
Soil	0.05	0.4	17.2	35	0	-------	--------

Table 1. Material properties for pile and soil

Following the definitions taken by [Konagai et. al. 2003], the point where 3% of the pile head deflection is reached determined the active length. Fig. 3 describes the variations with increasing frequency of the dynamic active pile length L_a normalized by its static value. Frequency, ω, is normalized with the single pile diameter, d, and the soil deposit shear wave velocity, v_s.

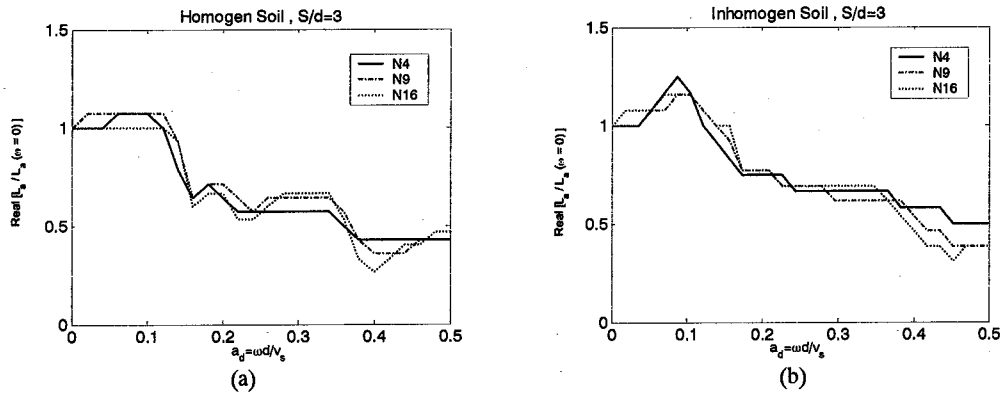

Fig. 3. Active pile length distribution against frequency factor, a_d, for different Pile-group configuration with S/d=3 located in Homogeneous (a) and Inhomogeneous (b) soil

Fig. 3 depicts that the curves are less sensitive to the change in number of piles, n_p. Fig. 4 shows variations of far-end displacements with respect to the depth, where I_f is the far-end displacement u_{far} normalized by its value at the ground surface level, $u_{far}(z=0)$. Figure 5 combines all the results for the examined soil pile-group cases. This confirms that the far end displacement $\{\mathbf{u}_{far}\}$ can be uniquely described as a function of the normalized depth z/L_a for a monotonic loading at the pile cap.

Figure 6 elucidates far-end displacements for the dynamic loading, the upper three and the lower three for the homogeneous and heterogeneous soil profiles, respectively. As the non-dimensional frequency increases, the displacements at deeper locations became larger. This tendency is clearer for narrower pile spaces. Curves for narrower pile spaces were plotted on one figure frame (Fig. 7). Frequency here was normalized by L_a and v_s in such a way that the non-dimensional frequency a_L indicates the ratio between the active pile length and the shear wave length in soils. This figure thus provides a perspective on the limitation of the proposed idea for describing the dynamic far-end displacement distribution with depth. However for the most important range of frequency ($a_L < 2$), far field soil displacement u_{far} can be practically expressed as a unique function of the active pile length L_a.

Fig. 7-c and 7-d describe imaginary part of the far-end displacement. Though with increase in non-dimensional frequency, the imaginary part at deeper locations became bigger but their values are almost small for the upper locations close to the ground surface. Since the main concern in seismic pile design goes into its upper part, therefore it is possible to ignore the effect of imaginary part in the far-end displacement with an enough approximation.

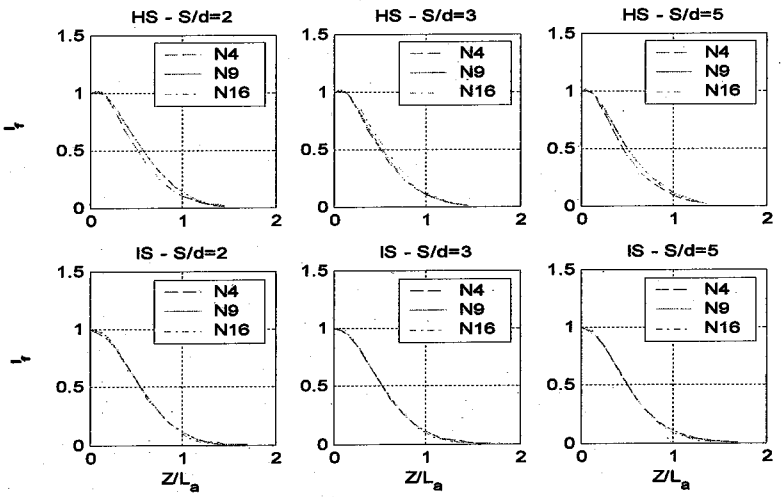

Fig. 4. Off-diagonal effect in terms of normalized depth for Homogenous soil, HS, and Inhomogeneous soil, IS, in Static state for different spacing ration among piles in the group

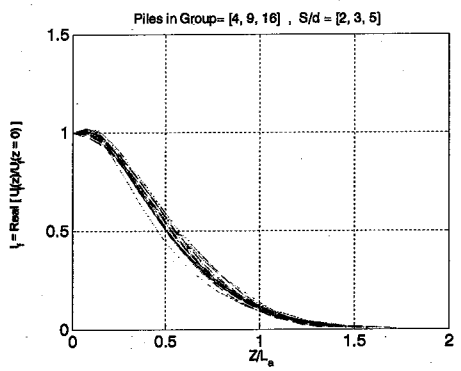

Fig. 5. All Off-diagonal representative effects together in terms of normalized depth For Homogenous and Inhomogeneous soil in Static state

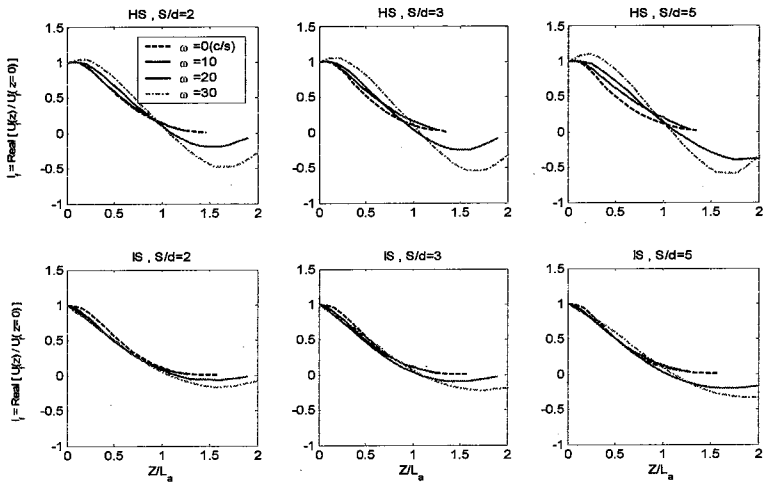

Fig. 6. Far-field representative effect in terms of normalized depth for Homogenous soil, HS, and Inhomogeneous soil, IS, in several frequencies and different spacing ration for a 3 by 3 pile-group

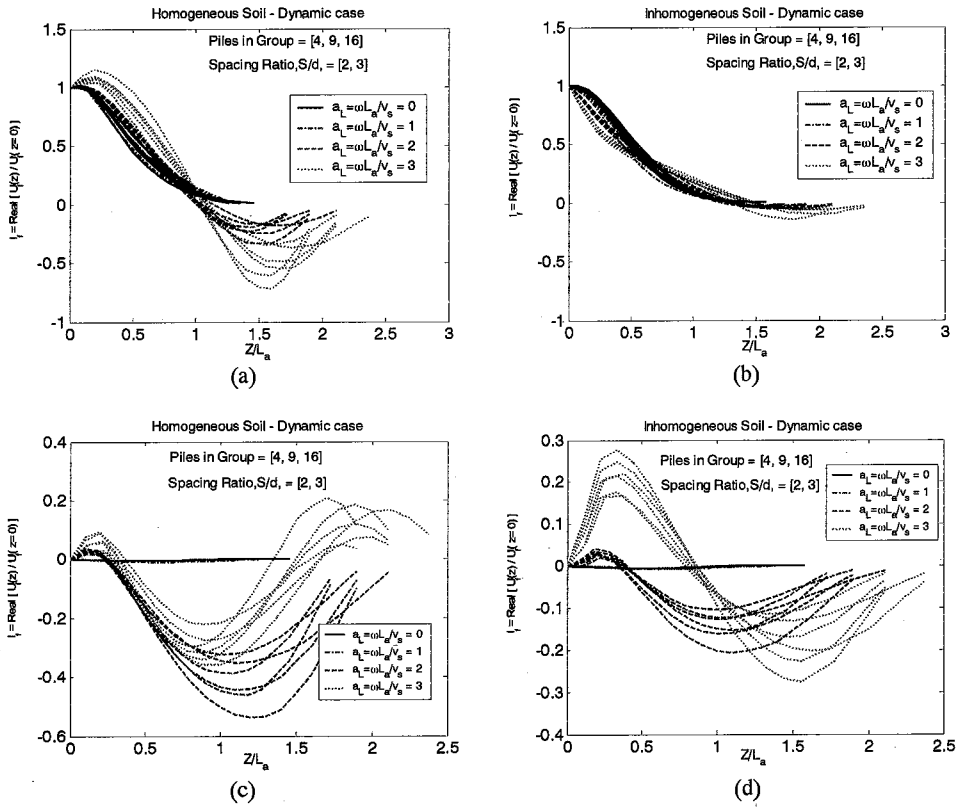

Fig. 7. Influence of frequency factor, a_L, on far-field representative parameter in terms of normalized depth for Homogeneous (a) and Inhomogeneous (b) soil

Nonlinear soil-pile interaction analysis

Taking the advantage of the modified Winkler model, a pushover analysis of a pile foundation subjected to lateral loading was conducted, and the result was compared with a rigorous solution obtained from an object-oriented OpenSees Finite Element Platform.

Material parameters of the pile and the soil are given in Table 2. The top 2.4m of the 13.7m long aluminum pile with a 0.429m * 0.429m square cross-section was assumed to stick out above the ground surface (see Fig. 8).

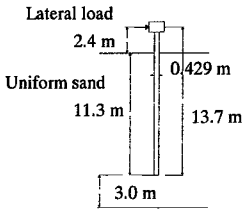

	Young modulus E (GPa)	Poisson ration, ν	Unit weight γ (KN/m^3)	Friction angle ϕ (deg)
Pile	69	0.33	26.5	------
Soil	Eq. (7)	0.35	14.5	37.1

Table 2. Material properties for pile and soil (McVay et al. 1998)

Fig. 8. Layout of Single Pile (Zhang et. al.1999)

The elastic modulus E of the medium dense sand was assumed to vary with confining pressure as:

$$E = E_0 \left[\sqrt[n]{(p/p_a)}\right] \qquad (p = \sigma_{ii}/3 = [(1+2k_0)\sigma_v'(z)]/3) \tag{7}$$

where, E_0 is the elastic modulus of soil under the atmospheric pressure (E_0=17.4 GPa, p_a=98 kPa), $\sigma_v'(z)$ is an effective overburden stress at the depth z, k_0 is the coefficient of earth pressure at rest estimated by a typical empirical equation $k_0 = 1 - \sin\phi$ with ϕ as the internal friction angle, and n is constant for a given void ratio, which was set at 2.0.

The pile model consists of 16 beam-column elements. Its bottom end was assumed to be fixed upright, while two boundary conditions were discussed for the top end of the pile. Elasto-plastic features of the side soil springs were assumed. The linear stiffness of each spring was identical to the corresponding diagonal component of the rigorous soil stiffness matrix described in the previous section, while its ultimate strength was given by:

$$Pu = \zeta \times (Kp - Ka) \times \gamma \times z = \zeta \times (1 - \frac{Ka}{Kp}) Kp\gamma\ z = \alpha_p Kp\gamma\ z \tag{8}$$

where, γ is the unit weight of soil, Ka and Kp are the active and passive earth pressure coefficients, ζ is a modification factor to represent three dimensional effects in the effective interaction zone in subsoil layers . Based on numerical results of various cases, $\alpha_p = 4$ was chosen (Shirato, M. 2004).

The effect of off-diagonal terms was taken into account just by adding the far-end soil displacements as has been mentioned above.

Finite element model

A complete 3D soil-pile model was created in OpenSees finite element framework. Taking account of its symmetric geometry, only half of the soil-pile system was realized (Fig. 9). The sand was assumed to follow the simple Drucker-Prager criterion with non-associated flow rule, and the soil strength was pressure-dependent. A self-weight analysis, in which, both the soil and the pile mass are subject to static gravitational loading, was thus necessary to realize the initial stress condition in the model. Then a push over analysis followed. In this analysis, lateral load applied to the pile head was increased stepwise.

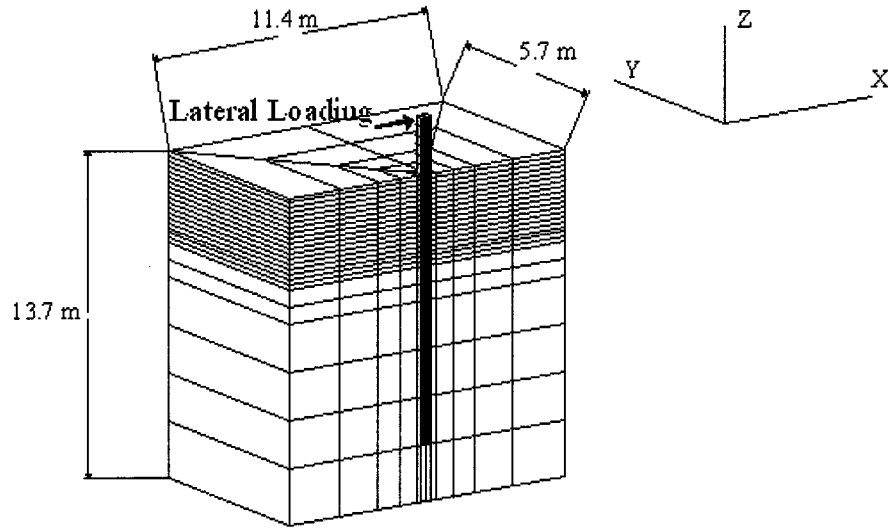

Fig. 9. Three dimensional FE mesh

Excluding the symmetric boundary, where only the vertical components of displacement were confined, three sides and the bottom of the soil medium were fixed. The interface layer between the aluminum pile and the surrounding soil was expressed by covering up the pile with thin layers of frictional brick elements. All the interface elements were assumed to follow the Drucker-Prager criterion with a friction angle of 25 *degrees*. Its dilation angle was set at zero.
The cross-section of the square pile was divided into four elements.

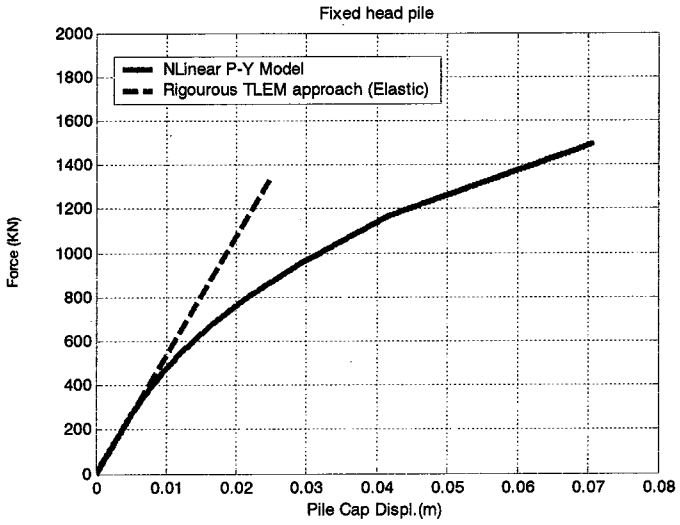

Fig. 10. Force-Displacement distribution of pile without free length on the ground

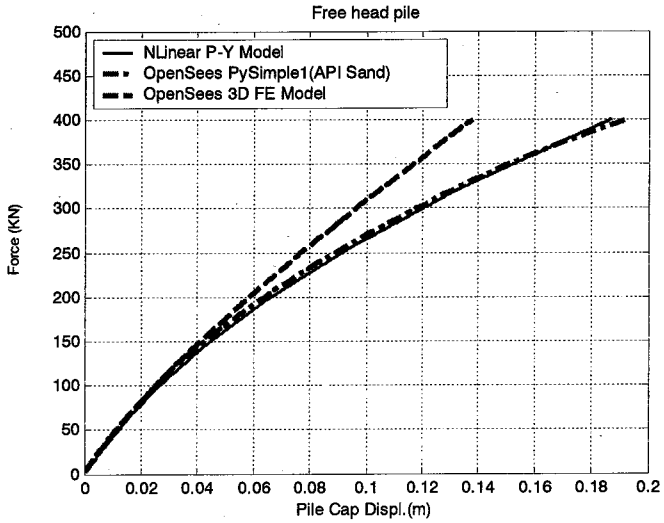

Fig. 11. Force-Displacement distribution of pile including free length on the ground

Fig. 10 compares the results from the present Winkler model and TLEM . A very good agreement in the initial elastic parts verifies the present approach. Fig. 11 shows p-y curves obtained from three different numerical models, which include, in addition to those aforementioned, the result from the OpenSees Py-Simple-1 model based on back bone curve proposed by the American Petroleum Institute (API), for sand materials (Boulanger RW et. al. 1999). A good correlation shows the potential of the proposed Modified Winkler Model for non-linear soil-pile group interaction analysis.

Conclusion

A new perspective for the soil-pile interaction analysis was provided in a way that the classical continuum mechanics theory yields a Winkler type expression of side soil stiffness. With the advantage of distinct expression of side soil stiffness at a particular depth, one can easily incorporate the effect of nonlinear soil behavior in the vicinity of a pile. With the present approach, obtained results showed good agreements with rigorous 3D solutions in both linear and nonlinear pushover analyses. The method still needs to be verified in cyclic loading cases, where gap creation among piles will affect the overall behaviors of soil-pile systems. The discussion will appear in future publications.

Acknowledgement

This work was primarily supported by the Ministry of Science, Research and Technology, MSRT, of the Iranian government under the Award of PhD scholarship for study on abroad.

References

1. American Petroleum Institute (API) "Recommended Practice for Planning, Designing, and Constructing Fixed Offshore Platforms", 1993, Washington, D.C.: API Recommended Practice 2A (RP2A).

2. Banerjee, P. K. and Sen, R. "Dynamic Behavior of Axially and Laterally Loaded Piles and Piles Group", 1987, Developments in Soil Mech. Found. Eng., Vol.3: 95-133.

3. Boulanger RW, Curras CJ, Kutter BL, Wilson DW, Abghari A. "Seismic Soil-Pile-Structure Interaction Experiments and Analyses", Journal of Geotechnical & Geoenvironmental Engineering, ASCE, 125(9), 1999: 750-759.

4. Jeremic B. and Yang Z. "Template Elastic Plastic Computations in Geomechanics", Int. J. for Numerical and Analytical Methods in Geomechanics, 2001, 01:1-6.

5. Kaynia A, Kausel E. "Dynamic Stiffness and Seismic Response of Pile Groups", NSF report, NSF/CEE -82023, 1982.

6. Kimura M, Zhang F. "Seismic Evaluations of Pile Foundations with Three Different Methods Based on Three-Dimensional Elasto-Plastic Finite Element Analysis", Soils and Foundations, 2000, 40(5): 113-132.

7. Konagai K. and Ahsan R. "Simulation of nonlinear SSI on a shaking table" Journal of Earthquake Engineering, Vol. 6, No. 1(2002) 31-51.

8. Konagai K, Ahsan R, Maruyama D. "Simple expression of the dynamic stiffness of grouped piles in sway motion", J Earthquake Eng. 2000; 4(3): 355–76.

9. Konagai K., Yin Y., Murono Y. "Single beam analogy for describing soil-pile group interaction" Soil Dynamic and Earthquake Eng. 2003, 23: 1-9.

10. Limin Zhang, M. M., and Lai, P. "Numerical analysis of laterally loaded 3x3 to 7x3 pile groups in sands", Journal of Geotechnical and Geoenvironmental Engineering, 1999, 125, 11: 936-946.

11. McVay, M., Zhang, L., Molnit, T., and Lai, P. "Centrifuge testing of large laterally loaded pile groups in sands", Journal of Geotechnical and Geoenvironmental Engineering, 1998, 124, 10: 1016-1026.

12. Nogami T., Otani J, Konagai K, Chen HL "Nonlinear Soil-Pile Interaction Model for Dynamic Lateral Motion", Journal of Geotechnical Engineering, ASCE, 118(1), 1992: 89-106.

13. OpenSees: Open System for Earthquake Engineering Simulation, 2004, Nov.30, (http://opensees.berkeley.edu/)

14. Poulos H. G. "Behavior of laterally loaded piles, part two" Journal of the Soil Mechanics and Foundations Division, ASCE, 97(SM5), 1971: 733-751.

15. Railway Technology Research Institute "Report of Field Tests of Prototype Pile Foundations", Tokyo, Japan, 1995, In Japanese.

16. Shirato, M. "Computational seismic performance assessment of a pile foundation subjected to a sever earthquake," PhD dissertation, Department of Civil Engineering, The University of Tokyo, 2004.

17. Tajimi H, Shimomura Y. "Dynamic Analysis of Soil-Structure Interaction by the Thin Layered Element Method" (in Japanese), 1976, Transactions of the Architectural Institute of Japan, Vol. 243: 41-51.

18. Wakai A, Gose S, Ugai K "3-D Elasto-Plastic Finite Element Analyses of Pile Foundations Subjected to Lateral Loading", Soils and Foundations, 1999, 39 (1): 97-11.

19. Yang Z., Jeremic B. "Numerical study of group effects for pile groups in sands" Int. J. for Numerical and Analytical Methods in Geomechanics, 2003, 27:1255–1276.